

Nonlinear Control Design for Maximum Power Point Tracking and Unity Power Factor of a Grid-Connected Photovoltaic Renewable Energy Systems

M. Guisser^{1*}, M. Aboufatah¹, E. Abdelmounim¹, H. Medromi², J. Saadi²

^{1*}(Department of Electrical Engineering, CRMEF-Settat, ASTI Laboratory, FST-Settat, University Hassan I, Morocco)

¹(ASTI Laboratory, FST-Settat, University Hassan I, Morocco)

²(LISER Laboratory, ENSEM-Casa, University Hassan II Ain-Chok, Morocco)

Abstract: This paper deals with the design of a nonlinear controller for single-phase grid-connected photovoltaic (PV) renewable energy systems to maintain the current injected into the grid in phase with grid voltage and to regulate the DC link voltage and to extract maximum power point tracking (MPPT). The system configuration includes a photovoltaic generator, DC-DC converter, DC-AC inverter coupled to grid network. The controller is designed using the backstepping control to optimize the PV energy extraction and to achieve unity power factor, the controller is based on an averaged nonlinear state space model of the controlled system. This is carried out via controlling the duty ratio of the DC-DC converter and DC-AC inverter. An integral action was added in order to robustify the controller with respect to parameter variations and disturbances. The synthesis of the regulator was achieved by having recourse to advanced tools of nonlinear control such as asymptotic stability in the sense of Lyapunov. The performance of the proposed controller is evaluated through numerical simulation in terms of delivering maximum power and synchronization of grid current with grid voltage under changes in atmospheric conditions.

Keywords: Grid-connected photovoltaic systems, Maximum power point tracking (MPPT), Unity power factor, Backstepping controller, Asymptotic stability.

I. Introduction

Solar energy has no noise and no pollution and is sustainable with a series of advantages. It has become one of the most potential green energies for development. Photovoltaic renewable energy sources has been initially used in stand-alone applications, nevertheless, PV systems that supply energy directly to the utility grid are becoming more popular because of the cost reduction due to the lack of a battery subsystem. Moreover, governmental laws and policies recently created that favors grid-connected PV systems have proved to be ineffective way to encourage the use of solar energy. Photovoltaic grid-connected system needs to use the grid-connected inverter as power conversion device of the DC output of the PV array into AC power.

Grid-connected PV systems still have many technical problems to be solved. Firstly, since the output power of the solar cell is easily influenced by environmental factors with obvious nonlinear factor, the photovoltaic cell is a very unstable power supply, so designing an efficient and reliable maximum power tracking control strategy is required to match the PV panel power to the irradiation and temperature changes. Many algorithms have been developed for tracking maximum point of a PV panel such as Perturb and Observation [1], and Incremental Conductance [2], neural network [3], fuzzy logic control [4] and sliding mode controller [5], [6], [7], [8]. Secondly, since the inverter is running excessive harmonic currents injected into the grid, the power system harmonic pollution problem is getting worse. Grid system becomes abnormal and false, and another equipment is also adversely affected, so various control strategy is proposed to solve this problem; power controlled [9], current controlled grid connected PV system [10] and hysteresis current control [11].

In this paper, a backstepping control strategy is developed to track the maximum power of the PV array and to synchronize the grid current with the grid voltage by ensuring the tight regulation of the DC-bus voltage and further reduce the harmonic content of the network current. The concept is to calculate an appropriate control law to guarantee the global asymptotic stability of the closed loop system. The control inputs of the grid-connected PV system are the duty cycles of the DC-DC converter and DC-AC inverter. The control input of the DC-DC converter achieves the maximum power point tracking, according to atmospheric condition changes. The control input of the DC-AC inverter achieves the unity power factor with regulation of the DC-link voltage and assure that the output current presents both low harmonic distortion and robustness in front of system's perturbations.

II. Grid-Connected PV System Modelling

The configuration of single-phase grid-connected photovoltaic system is shown in Fig.1. It consists of PV array connected to the DC bus via a DC-DC boost converter, and then to the AC grid via a DC-AC inverter. The boost converter is used for boosting the array voltage and achieving maximum power point tracking for the PV array. The inverter with filter inductor converts a DC input voltage into an AC sinusoidal, by means of appropriate switch signals to make the output current in phase with the utility voltage and so obtain a power factor unity.

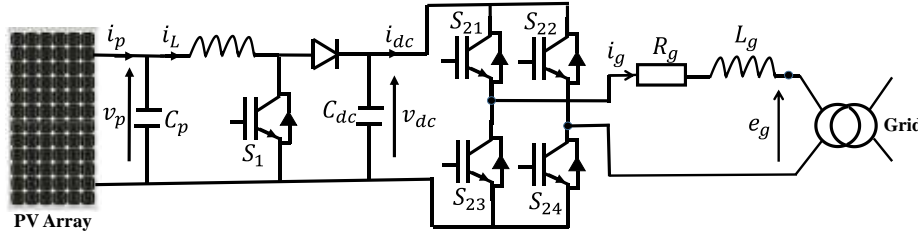


Fig. 1. Single-phase grid connected PV system.

2.1. Photovoltaic Array Modelling

Typically, a PV cell is a simple p-n junction diode, which converts solar irradiation into electricity. Fig. 2 illustrates a simple equivalent circuit diagram of a PV cell. This model consists of a current source I_{ph} which represents the light generated current from PV cell, a diode in parallel with the current source, a shunt resistance R_{sh} , and a series resistance R_s .

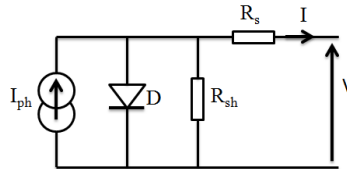


Fig. 2. Equivalent circuit of a PV cell.

The terminal equation for the PV current i_p and PV voltage v_p of the solar cell is given as follows:

$$i_p = I_{ph} - I_s \left[\exp\left(\frac{v_p + R_s i_p}{\gamma V_T}\right) - 1 \right] - \frac{v_p + R_s i_p}{R_{sh}} \quad (1)$$

where I_s is the saturation current, $V_T = K_B T/q$ is the thermal voltage, K_B is the Boltzmann's constant, q is the charge of electron, T is the cell's absolute working temperature, γ is the p-n junction ideality factors. The light generated current I_{ph} depends on the solar irradiation and temperature, which can be related by the following equation:

$$I_{ph} = [I_{scr} + K_i(T - T_r)] \frac{G}{1000} \quad (2)$$

where, I_{scr} is the short circuit current, G is the solar irradiation, K_i is the cell's short circuit current coefficient and $T_r = 298.15K$ is the reference temperature of the cell. The cell's saturation current I_s varies with the temperature according to the following equation:

$$I_s = I_{rr} \left[\frac{T}{T_r} \right]^3 \left[\exp\left(\frac{qE_G}{\gamma K_B} \left(\frac{1}{T_r} - \frac{1}{T} \right) \right) \right] \quad (3)$$

where, E_G is the band-gap energy of the semiconductor used in the cell and I_{rr} is the reverse saturation current of the cell at reference temperature and solar irradiation.

PV cells, usually considered to have the same characteristics, are arranged together in series and parallel to form arrays in order to obtain a high voltage and current. The mathematical equation relating the PV array current to the PV array voltage becomes:

$$i_p = N_p I_{ph} - N_p I_s \left[\exp\left(\frac{1}{\gamma V_T} \left(\frac{v_p}{N_s} + \frac{R_s i_p}{N_p} \right) - 1 \right) \right] - \frac{N_p}{R_{sh}} \left(\frac{v_p}{N_s} + \frac{R_s i_p}{N_p} \right) \quad (4)$$

where N_s is the number of cells in series and N_p is the number of modules in parallel.

The PV array considered in this paper is the Siemens SM55. The corresponding electrical characteristics are listed in Table 1.

Nominal voltage	12V
Maximum power	55W
Current at the maximum power point	3.15A
Voltage at the maximum power point	17.4V

Maximum current (short circuit output)	3.45A
Maximum voltage (open circuit)	21.7V
Current temperature coefficient	+1.2mA/°C
Number of series cells N_s	36
Number of parallel modules N_p	1

Table 1: Parameter values of the PV array Siemens SM55.

Figs. 3 and 4 show the constitutive curves of the PV array for different values of temperature and solar incident irradiance. Two important electrical characteristics of the PV array are observed in those figures: That there is an operating point, marked in the figures, in which the PV array generates more power than the other points. That there are different maximum power points for each curve. The aforementioned observations imply that during one day the maximum power point of a PV array varies according to the solar incident irradiance and temperature changes.

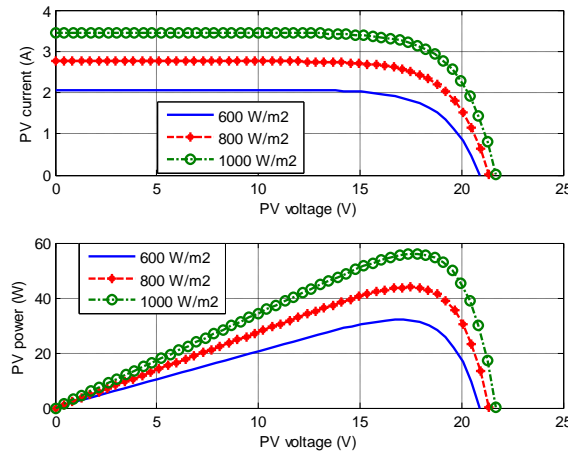


Fig. 3. PV array current–voltage and PV array power–voltage at 25°C at different irradiance levels.

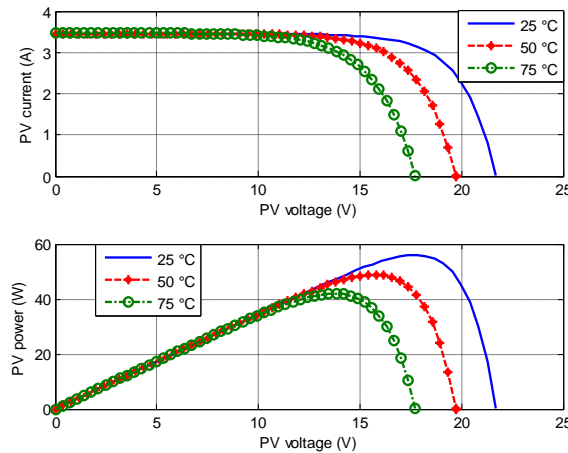


Fig. 4. PV array current–voltage and PV array power–voltage at 1000W/m² at different temperature levels.

Based on the solar array characteristic curves shown in Figs. 3 and 4, it can be found that a maximum power point occurs when the derivative of PV output power $P = v_p i_p$ with respect to terminal voltage v_p equals zero. Therefore:

$$\left. \frac{\partial P}{\partial v_p} \right|_{MPP} = \frac{\partial (v_p i_p)}{\partial v_p} = i_p + v_p \frac{\partial i_p}{\partial v_p} = 0 \quad (5)$$

2.2. Single-phase Grid-connected PV System Modelling

The power converter structure used to interface the photovoltaic array with the power grid as shown in Fig 2. In the specific architecture considered in this work, the PV panel is connected to the input of a single full-bridge power inverter by means of a DC-DC converter and a DC-link capacitor. The DC-DC boost converter consists of the switch S_1 controlled by a switching signal $\mu_1 \in \{0, 1\}$ (i.e., OFF or ON respectively) and the full-bridge inverter consists of four switches $\{S_{21}, S_{22}, S_{23}, S_{24}\}$ controlled by a switching signal $\mu_2 \in \{0, 1\}$. The

switching signal μ_1 and μ_2 can also be generated via a pulse-width modulator (PWM) scheme with an input signal $u_i (i = 1, 2) \in [0, 1]$ outputted by the controller. In this case, if the switching frequency is sufficiently high, the dynamical behavior of the PV system can be approximated by the following set of differential equations:

$$\begin{cases} \frac{dv_p}{dt} = \frac{1}{C_p} i_p - \frac{1}{C_p} i_L \\ \frac{di_L}{dt} = \frac{1}{L} v_p - \frac{1}{L} (1 - u_1) v_{dc} \\ \frac{dv_{dc}}{dt} = \frac{1}{C_{dc}} (1 - u_1) i_L + \frac{1}{C_{dc}} (1 - 2u_2) i_g \\ \frac{di_g}{dt} = -\frac{1}{L_g} R_g i_g - \frac{1}{L_g} e_g - \frac{1}{L_g} (1 - 2u_2) v_{dc} \\ y_1 = \frac{\partial P}{\partial v_p} = i_p + v_p \frac{\partial i_p}{\partial v_p} \\ y_2 = i_g \end{cases} \quad (6)$$

where C_p is the input capacitor and L is the inductor of the boost converter. C_{dc} is the DC link capacitor, L_g is the filter inductor and R_g is the equivalent series resistance of the filter inductor. i_p , v_p , i_L , v_{dc} , i_g and e_g are respectively, the average values over switching period of the PV array current, PV array voltage, boost inductor current, DC bus voltage, grid current and grid voltage, y_1 and y_2 are the controlled outputs of the power system. The control inputs u_1 and u_2 are the average values (duty cycles) of the binary input switching signals μ_1 and μ_2 . The utility grid voltage $e_g = A \sin(\omega t)$ is assumed to be sinusoidal with a constant amplitude A and a constant frequency $\omega = 2\pi f$.

III. Controller Design

The control strategy of the power converter and power inverter that interface the PV array with the utility grid needs to accomplish the following control objectives in order to assure an efficient energy transfer:

- The maximum power extraction from the PV array by means of tracking the solar array maximum power point (MPP) that varies with the solar irradiance and the PV array temperature.
- The proper conversion of the DC input power into an AC output current, which has to be injected to the grid. This current has to exhibit low harmonic contents and must be in phase to the grid voltage in order to perform the power transfer at unity power factor.
- The tight regulation of the DC-bus voltage.

To accomplish the previous objectives, a nonlinear controller is developed using the backstepping technique based on the averaged nonlinear state space model of the controlled system. The proposed control system will have the structure shown in Fig.5. The MPPT controller and unity power factor controller will be synthesized using backstepping approach [12], [13], [14], [15] and the third will be done by a simple proportional-integral corrector.

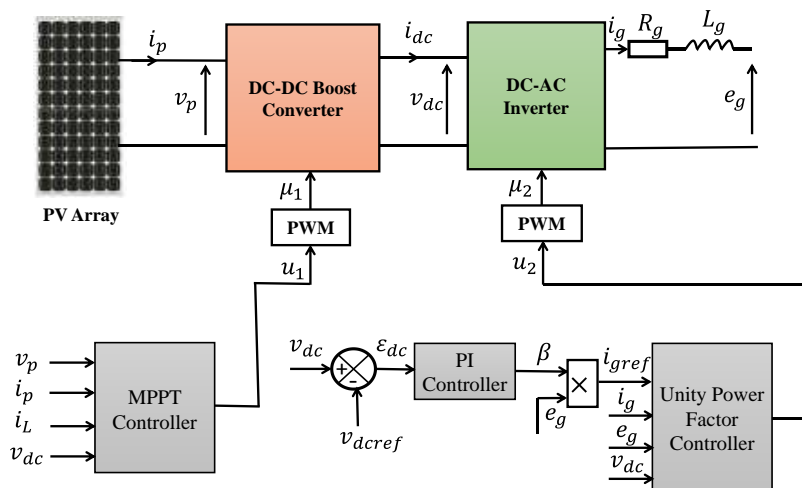


Fig. 5. Control scheme of the grid-connected PV system.

3.1. MPPT Controller

The maximum power point tracking control has to settle the PV array operating point at its maximum power value for any temperature and irradiance variation, by means of the input signal u_1 that controls

the switch of the boost converter. The control objective is to regulate the controlled output $y_1 = \frac{\partial P}{\partial v_p}$ of the photovoltaic array to its reference $y_{1ref} = \frac{\partial P}{\partial v_p} \Big|_{MPP} = 0$.

Backstepping design procedure:

Design Step: Let us introduce the following tracking error $\varepsilon_1 = y_1 - y_{1ref}$ and including integral action $\xi_1(t) = \int_0^t (y_1(\tau) - y_{1ref}(\tau)) d\tau$.

Deriving ε_1 with respect to time and accounting for (5) and (6), implies:

$$\dot{\varepsilon}_1 = \frac{1}{C_p} \left(2 \frac{\partial i_p}{\partial v_p} + v_p \frac{\partial^2 i_p}{\partial v_p^2} \right) (i_p - i_L) \quad (7)$$

Treating the boost inductor current i_L as a virtual control signal for (7) and considering the first Lyapunov function positive definite:

$$V_1(\xi_1, \varepsilon_1) = \frac{1}{2} \xi_1^2 + \frac{1}{2} \varepsilon_1^2 \quad (8)$$

The derivative of V_1 with respect to time, is given by:

$$\dot{V}_1 = \varepsilon_1 \left[\dot{\xi}_1 + \frac{1}{C_p} \left(2 \frac{\partial i_p}{\partial v_p} + v_p \frac{\partial^2 i_p}{\partial v_p^2} \right) (i_p - i_L) \right] \quad (9)$$

As i_L is just a state variable and not an effective control input, the stabilization of ξ_1 and ε_1 can be obtained by introducing a new virtual control $\alpha_1 = (i_L)_d$, where $(i_L)_d$ is the desired value of the boost inductor current. The virtual control law would be:

$$\xi_1 + \frac{1}{C_p} \left(2 \frac{\partial i_p}{\partial v_p} + v_p \frac{\partial^2 i_p}{\partial v_p^2} \right) (i_p - \alpha_1) = -k_1 \varepsilon_1 \quad (10)$$

Where $k_1 > 0$ being a design parameter. The desired value α_1 is called a stabilization function, is given by:

$$\alpha_1 = i_p + \frac{C_p}{2 \frac{\partial i_p}{\partial v_p} + v_p \frac{\partial^2 i_p}{\partial v_p^2}} (k_1 \varepsilon_1 + \xi_1) \quad (11)$$

The Lyapunov candidate function whose dynamics is negative definite: $\dot{V}_1 = -k_1 \varepsilon_1^2 < 0$.

Design Step 2: We define the following second error variable of the boost inductor current error $\varepsilon_2 = i_L - \alpha_1$, where the inductor current should reach the desired value α_1 to make the error vanish in order to achieve the control aim. The time derivative of this error is:

$$\dot{\varepsilon}_2 = \frac{di_L}{dt} - \dot{\alpha}_1 = \frac{1}{L} (v_p - (1 - u_1)v_{dc}) - \dot{\alpha}_1 \quad (12)$$

Substituting $i_L = \varepsilon_2 + \alpha_1$ into equation (7), $\dot{\varepsilon}_1$ becomes:

$$\dot{\varepsilon}_1 = \frac{1}{C_p} \left(2 \frac{\partial i_p}{\partial v_p} + v_p \frac{\partial^2 i_p}{\partial v_p^2} \right) (i_p - \varepsilon_2 - \alpha_1) \quad (13)$$

Introducing (11), we obtain the time derivative of ε_1 and V_1 :

$$\dot{\varepsilon}_1 = -k_1 \varepsilon_1 - \xi_1 - \frac{1}{C_p} \left(2 \frac{\partial i_p}{\partial v_p} + v_p \frac{\partial^2 i_p}{\partial v_p^2} \right) \varepsilon_2 \quad (14)$$

$$\dot{V}_1 = -k_1 \varepsilon_1^2 - \frac{1}{C_p} \left(2 \frac{\partial i_p}{\partial v_p} + v_p \frac{\partial^2 i_p}{\partial v_p^2} \right) \varepsilon_1 \varepsilon_2 \quad (15)$$

The time derivative of the stabilising function α_1 is given by:

$$\dot{\alpha}_1 = \left[\frac{\partial i_p}{\partial v_p} \frac{\partial v_p}{\partial t} + C_p \left(\frac{(k_1 \varepsilon_1 + \xi_1)}{\left(2 \frac{\partial i_p}{\partial v_p} + v_p \frac{\partial^2 i_p}{\partial v_p^2} \right)} - \frac{(k_1 \varepsilon_1 + \xi_1)}{\left(2 \frac{\partial i_p}{\partial v_p} + v_p \frac{\partial^2 i_p}{\partial v_p^2} \right)^2} \left(3 \frac{\partial^2 i_p}{\partial v_p^2} + v_p \frac{\partial^3 i_p}{\partial v_p^3} \right) \frac{\partial v_p}{\partial t} \right) \right] \quad (16)$$

Consider the augmented Lyapunov function candidate:

$$V_2(\xi_1, \varepsilon_1, \varepsilon_2) = V_1 + \frac{1}{2} \varepsilon_2^2 \quad (17)$$

The time derivative of the second Lyapunov function is obtained by combining equations (12) and (15):

$$\dot{V}_2 = -k_1 \varepsilon_1^2 + \varepsilon_2 \left[-\frac{1}{C_p} \left(2 \frac{\partial i_p}{\partial v_p} + v_p \frac{\partial^2 i_p}{\partial v_p^2} \right) \varepsilon_1 + \frac{1}{L} (v_p - v_{dc}) + \frac{1}{L} u_1 v_{dc} - \dot{\alpha}_1 \right] \quad (18)$$

The control law u_1 which guarantees the negativity of the dynamics of the Lyapunov candidate function V_2 , is given by:

$$u_1 = \frac{L}{v_{dc}} \left[-k_2 \varepsilon_2 + \frac{1}{C_p} \left(2 \frac{\partial i_p}{\partial v_p} + v_p \frac{\partial^2 i_p}{\partial v_p^2} \right) \varepsilon_1 - \frac{1}{L} (v_p - v_{dc}) + \dot{\alpha}_1 \right] \quad (19)$$

where $k_2 > 0$ is a positive constant. The above choice yields:

$$\dot{V}_2 = -k_1 \varepsilon_1^2 - k_2 \varepsilon_2^2 < 0 \quad (20)$$

which ensures that the state vector error $(\xi_1, \varepsilon_1, \varepsilon_2)$ converges asymptotically to the origin, which implies that $\varepsilon_1 = y_1 - y_{1ref} = \partial P / \partial v_p$ converges asymptotically to the origin. Therefore, the maximum power extraction from the PV array is achieved.

3.2. Unity Power Factor Controller

The unity power factor controller input signal u_2 that controls the inverter have been carried out by means of on two cascaded control loops, where the inner current control loop is in charge to establish the duty ratio for the generation of a sinusoidal output current in phase with the grid voltage and ensuring current harmonics rejection. In turn, the outer voltage control loop has to settle the DC bus voltage regulating at its desired value, this loop delivers to the inner control loop the current reference amplitude corresponding to the PV array maximum power, thereby ensuring the power transfer to the grid.

The inner controller allows the grid current i_g to track a reference signal i_{gref} of the form:

$$i_{gref} = \beta e_g = \beta A \sin(\omega t) \quad (21)$$

Where β is an adjustment positive parameter and it can be adjusted by a PI control.

Let us introduce the following tracking current error $\varepsilon_3 = y_2 - y_{2ref} = i_g - i_{gref}$. Its dynamics is given by:

$$\dot{\varepsilon}_3 = -\frac{1}{L_g} R_g i_g - \frac{1}{L_g} e_g - \frac{1}{L_g} (1 - 2u_2) v_{dc} - \frac{di_{gref}}{dt} \quad (22)$$

Let us use the Lyapunov candidate function by introducing the integral action $\xi_2(t) = \int_0^t (i_g(\tau) - i_{gref}(\tau)) d\tau$:

$$V_3(\xi_2, \varepsilon_3) = \frac{1}{2} \xi_2^2 + \frac{1}{2} \varepsilon_3^2 \quad (23)$$

As its derivative with respect to time, is given by:

$$\dot{V}_3 = \varepsilon_3 \left[\dot{\xi}_2 - \frac{1}{L_g} R_g i_g - \frac{1}{L_g} e_g - \frac{1}{L_g} (1 - 2u_2) v_{dc} - \frac{di_{gref}}{dt} \right] \quad (24)$$

The stabilizing control law by making \dot{V}_3 negative definite is given by:

$$u_2 = \frac{1}{2} \left[1 + \frac{1}{v_{dc}} \left(R_g i_g + e_g + L_g \left(\frac{di_{gref}}{dt} - k_3 \varepsilon_3 - \dot{\xi}_2 \right) \right) \right] \quad (25)$$

where $k_3 > 0$ is a positive parameter; which yields $\dot{V}_3 = -k_3 \varepsilon_3^2 < 0$, then the tracking error ε_3 converges asymptotically to zero. Therefore, the grid current is sinusoidal and in phase with the grid voltage.

The aim of the outer voltage loop is to design a variation law for the ratio β in equation (21) so that the inverter DC input voltage v_{dc} is steered to a given constant reference v_{dcref} . This regulator is given by the following PI control law:

$$\beta(t) = k_4 (v_{dc}(t) - v_{dcref}(t)) + k_5 \int_0^t (v_{dc}(\tau) - v_{dcref}(\tau)) d\tau \quad (26)$$

where k_4 and k_5 are respectively the proportional and integral gain.

IV. Simulation Results and Discussions

Numerical simulations were made in the Simulink/Matlab platform to verify the performance of the controller; all parameters of the photovoltaic system components and controller are depicted in Table 2. Two scenarios were simulated. In the first one, realistic variations were applied to the irradiance from 500 W/m^2 to 1000 W/m^2 at 0.5s while maintaining the cell temperature constant at 25°C . The resulting control performances are illustrated by Fig. 6 to Fig. 9. The reference DC bus voltage value is held at $v_{dcref} = 40 \text{ V}$. The second scenario was simulated for temperature changes from 25°C to 50°C at 0.5s while the radiation is constant equal to 1000 W/m^2 . The corresponding performances are illustrated by Fig. 10 to Fig. 13.

From these Figures, it is clear that the maximum power point is always reached very quickly with excellent accuracy and good performances according to atmospheric condition changes. The grid current is sinusoidal and in phase with the grid voltage, which proves the unity power factor achievement. Noting that the DC bus voltage is regulated to its desired value. In addition to that, this controller has to be used in order to achieve the synchronization to the grid and to perform the power management between the PV system and the electrical grid.

Photovoltaic array parameters	Boost converter, inverter and grid parameters	Controller parameters
$R_s = 0.1124 \Omega$	$C_p = 4700 \mu\text{F}$	$k_1 = 900$
$R_{sh} = 6500 \Omega$	$C_{dc} = 470 \mu\text{F}$	$k_2 = 900$
$\gamma = 1.7404$	$L = 3.5 \text{ mH}$	$k_3 = 200$
$I_{scr} = 3.45 \text{ A}$	$L_g = 2.2 \text{ mH}$	$k_4 = 0.01$
$I_{rr} = 4.842 \mu\text{A}$	$R_g = 0.7 \Omega$	$k_5 = 1$
$N_s = 36$	$A = 22\sqrt{2} \text{ V}; f = 50 \text{ Hz}$	
$N_p = 1$	$v_{dcref} = 40 \text{ V}$	

Table 2: Power system and controller parameters.

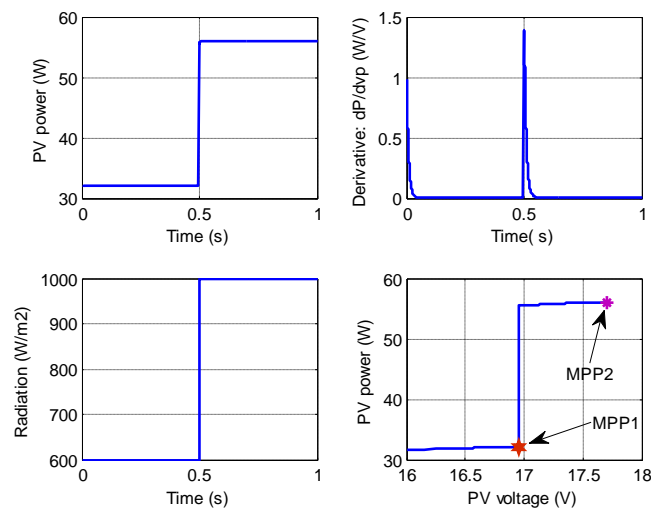


Fig. 6. PV power, controlled output, radiation and PV array power-voltage characteristic in presence of radiation changes.

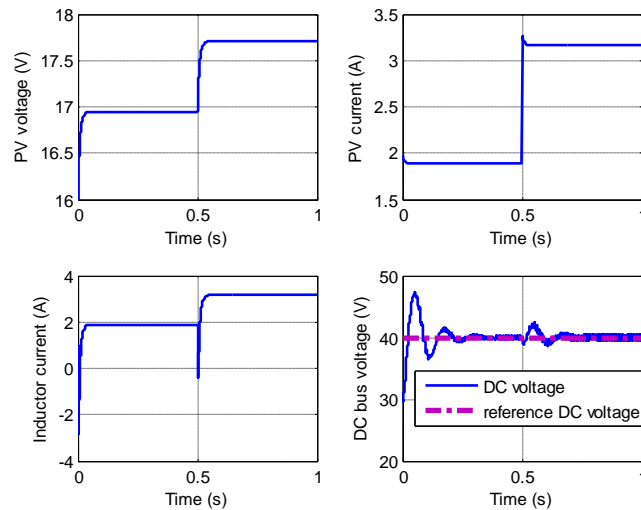


Fig. 7. PV array voltage, PV array current, boost inductor current and DC bus voltage in presence of radiation changes.

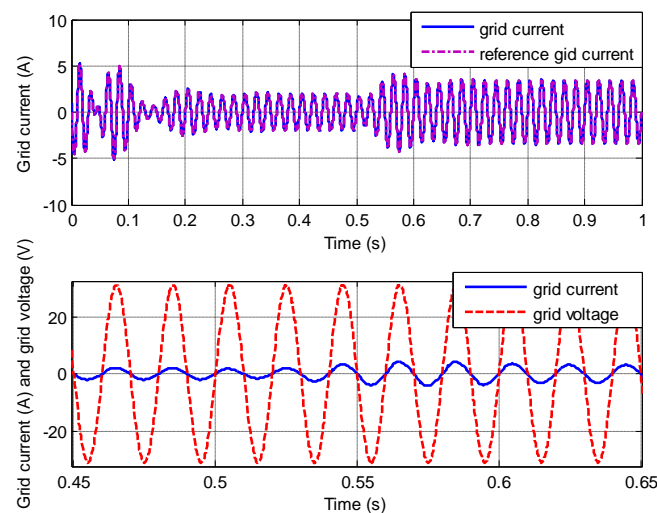


Fig. 8. Grid current and its reference and grid voltage in presence of radiation changes.

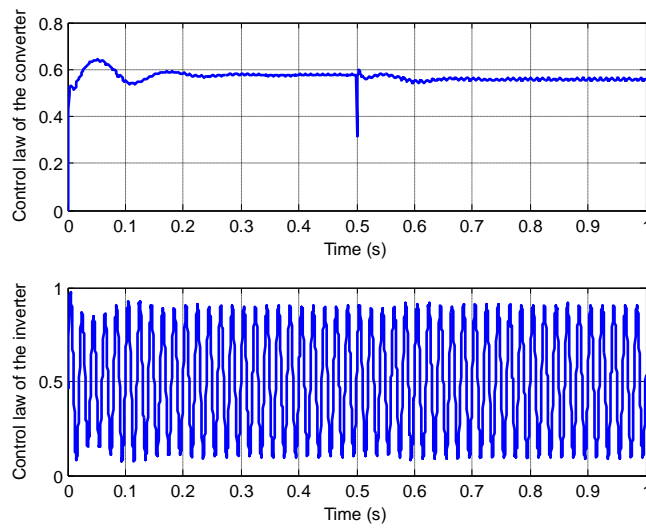


Fig. 9. Input controls of the converter and inverter in presence of radiation changes.

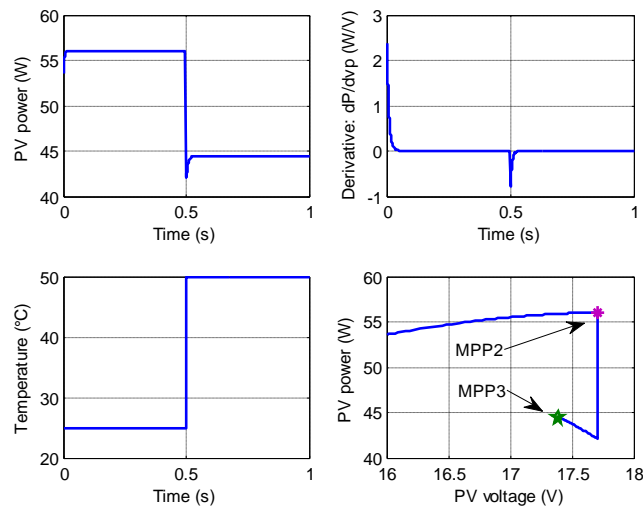


Fig. 10. PV power, controlled output, temperature and PV array power-voltage characteristic in presence of temperature changes.

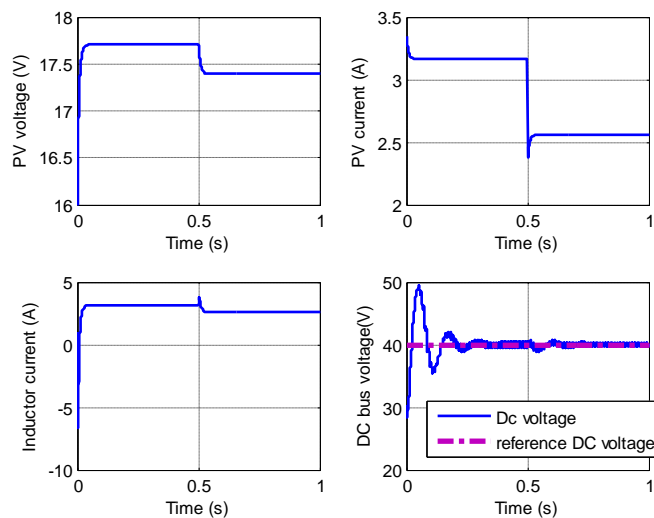


Fig. 11. PV array voltage, PV array current, boost inductor current and DC bus voltage in presence of temperature changes.

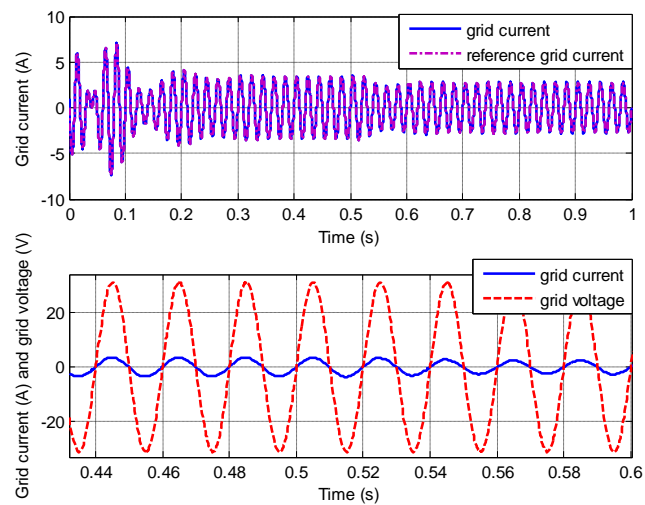


Fig. 12. Grid current and its reference and grid voltage in presence of temperature changes.

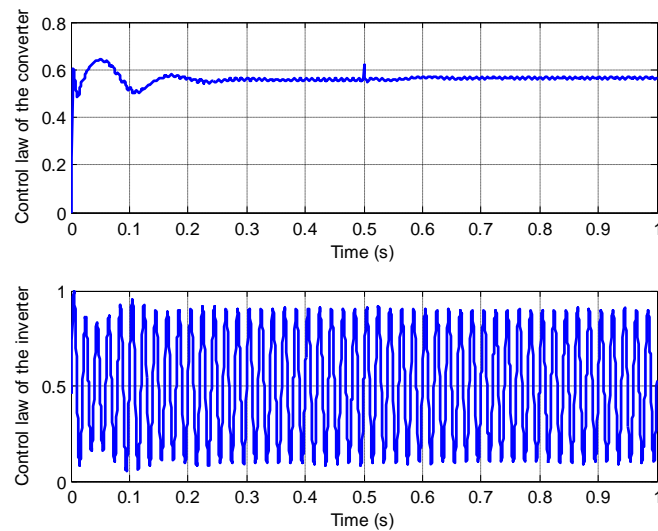


Fig. 13. Input controls of the converter and inverter in presence of temperature changes.

V. Conclusion

This paper presents a new nonlinear control strategy of single-phase grid-connected PV generation system. The controller is designed to extract maximum power from the PV array and to inject a sinusoidal current in the grid with unity power factor and regulating the DC bus voltage. The studied system is described by a representation of nonlinear state space average model. To track the designed trajectory, a tow backstepping controller and a proportional-integral corrector are developed to modulate the duty cycle of the interleaved boost converter and inverter. The controller is proven to yield asymptotic stability with respect to the tracking errors via Lyapunov analysis. The proposed controller has the advantages of robustness, accurate tracking, fast response and good performance. Simulation results, obtained under Matlab/Simulink environment, show the control performance and dynamic behavior of grid-connected photovoltaic system provides good results and show that the control system is robust and efficiency.

References

- [1] N. Femia, G. Petrone, G. Spagnuolo, and M. Vitelli, Optimization of Perturb and Observe maximum power point tracking method, *Power Electronics, IEEE Transactions*, Vol. 20, n.4, July 2005, pp. 963–973.
- [2] Jae Ho Lee; HyunSuBae; Bo Hyung Cho, Advanced Incremental Conductance MPPT Algorithm with a Variable Step Size, *Power Electronics and Motion Control Conference EPEPEMC 12th International*, Sept 2006, pp. 603 – 607.
- [3] A. Tariq and M. S. Jami Asghar, Development of an Analog Maximum Power Point Tracker for Photovoltaic Panel, *International IEEE Annual Conference on Power and Electronics and Drives Systems*, Vol.1, Jan. 2006, pp.251-255.
- [4] NoppornPatcharaprakiti, SuttichaiPremrudeepreechacharn, YosanaoSriuthaisiriwong, Maximum power point tracking using adaptive fuzzy logic control for grid-connected photovoltaic system, *Renewable Energy*, Vol 30 n.11, Sept 2005, pp. 1771–1778.

- [5] HazemFeshara, Mohamed Elharony, SolimanSharaf, Design, Digital Control, and Simulation of a GridConnected Photovoltaic Generation System. International Journal of Renewable Energy Research, Vol.4, No.2, 2014.
- [6] Jui-Liang, Ding-Tsair Su, Ying-ShingShiao, Research on MPPT and Single-Stage Grid-Connected for Photovoltaic System, Wseas Transactions on Systems, Volume 7, October 2008.
- [7] M. Guisser, A. EL-Jouni, EL. H. Abdelmounim, Robust Sliding Mode MPPT Controller Based on High Gain Observer of a Photovoltaic Water Pumping System, International Review of Automatic Control, Vol 7, No 2, 2014.
- [8] M'hammedGuisser, ElhassaneAbdelmounim, Mohammed Aboulfatah, Abdesselam EL-Jouni, Nonlinear Observer-Based Control for Grid Connected Photovoltaic System, IOSR Journal of Electrical and Electronics Engineering, Volume 9, 2014.
- [9] F. L. Albuquerque, A. J. Moraes, G. C. Guimarks, S. M. R. Sanhueza, optimization of a photovoltaic system connected to electric power grid, IEEE transaction and distribution conference and exposition, pp. 645-650. Latin American, 2004.
- [10] Jianxing Liu, Salah Laghrouche, MaximeWack, Observer-Based Higher Order Sliding Mode Control of Unity Power Factor in Three-Phase AC/DC Converter for Hybrid Electric Vehicle Applications, International Journal of Control, 2013.
- [11] G. He-rong, Y. Zi-long, W. Wu, Research on hysteresis band current tracking control of grid-connected inverter, Proceedings of the Chinese Society of Electrical Engineering, vol. 26, no.9, pp.108-112, 2006.
- [12] Krstić M., I. Kanellakopoulos, P. V. Kokotović. Nonlinear and adaptive control design. John Willy & Sons, NY, 1995.
- [13] Y. Tan, J. Chang, H. Tan, and J. Hu, Integral backstepping control and experimental implementation for motion system, in Proc. IEEE Int. Conf. Contr. Appl., (Anchorage, Alaska, USA), pp. 367-372, IEEE, Sept. 2000.
- [14] Roger Skjetne, Thor I. Fossen, On Integral Control in Backstepping: Analysis of Different Techniques, Proceeding of the American Control Conference Boston, Massachusetts June 30-July 2, 2004.
- [15] Chao-Chung Peng, Yunze Li and Chieh-Li Chen, A Robust Integral Type Backstepping Controller Design for Control of Uncertain Non Linear Systems subject to Disturbance, International Journal of Innovative Computing, Information and Control, Volume7, Number 5(A), May 2011.